A comparative analysis of the attribution of extreme summer precipitation in south and north parts of the East China monsoon region—with the year 2020 as an example

A comparative analysis of the attribution of extreme summer precipitation in south and north parts of the East China monsoon region - with the year 2020 as an example

Rouke Li [a, b, c], Xiaodong Liu [a, b], Ying Xu[c], Buwen Dong[d]

[a] State Key Laboratory of Loess and Quaternary Geology, Institute of Earth Environment, Chinese Academy of Sciences, Xi'an, 710061, China

[b] University of Chinese Academy of Sciences, Beijing, 100049, China

[c] National Climate Center, Beijing, 100081, China

[d] National Centre for Atmospheric Science, Department of Meteorology, University of Reading, Reading, United Kingdom

Correspondence

Rouke Li and Xiaodong Liu, State Key Laboratory of Loess and Quaternary Geology, Institute of Earth Environment, Chinese Academy of Sciences, Xi'an, 710061, China.

Email: lirk4321@163.com (R.L.) and liuxd@loess.llqg.ac.cn (X.L.)

Funding information

National Natural Science Foundation of China, Grant/Award Numbers: 41991254; China Three Gorges Corporation, Grant/Award Numbers: 0704081; key Youth Innovation Team of China Meteorological Administration, Grant/Award Numbers: CMA2023QN15.

Abstract

In summer 2020, several watersheds in China monsoon region experienced historically unusually heavy precipitation. The flooding associated with these heavy precipitation events led to devastating impacts on human life, infrastructure, agriculture, and economy. Using historical climate simulations from the HadGEM3-GA6 and CMIP6 models under influences of natural and/or anthropogenic forcings, we conducted a comparative study on the attribution of extremely heavy precipitation events in summer 2020 in the mid-lower reaches of the Yangtze River and the mid-lower reaches of the Yellow River- Hai River Basin which locates respectively in the south and north parts of the East China monsoon region. The potential contributions of anthropogenic forcings to monthly-scale extreme precipitation and daily maximum precipitation (RX1day) were examined. The results suggest that human activities have decreased the probability of month-scale extreme precipitation events in south part of the East China monsoon region. For RX1day extreme precipitation events, anthropogenic factors have increased their probability in both regions. However, the influence of anthropogenic forcings on month-scale extreme precipitation events in north part of the East China monsoon region is not robust among two attribution systems. Further analyses indicated that anthropogenic aerosols (AER) make both month-scale extreme precipitation events and extreme RX1day less likely to occur in summer 2020, and greenhouse gases (GHG) increase the likelihood of both. GHG influences on Rx1day overwhelm AER influences, leading to an increase of the probability of Rx1day similar to the 2020 events in both regions. In contrast, the decrease of the probability of month-scale precipitation in south part of the East China monsoon region is predominantly due to aerosol forcing. The model projections show that the likelihood of both monthly and daily extreme precipitation events in both regions will increase in the future. Accordingly, the recurrence period of extreme precipitation events will be shortened by the end of the 21st century, which is more significant under the high emission scenario.

KEYWORDS

East China monsoon region, extreme precipitation, attribution, future projection

1 INTRODUCTION

Since the industrial revolution, the global mean near-surface temperature has increased by about 1.10°C (0.97-1.25°C), resulting in multiple impacts on other climate system components, including increasingly frequent extreme weather events (IPCC, 2021). Observational studies suggest a strong link between climate warming and increased extreme precipitation at the global scale (Papalexiou and Montanari, 2019). Furthermore, extreme precipitation events have increased in many parts of China (Wang and Qian, 2009). Persistent heavy precipitation events that were anomalously greater than normal during the summer 2020 resulted in record-breaking precipitation in the Yangtze River catchment and the Yellow River catchment (China Meteorological Administration, 2021). According to the Ministry of Emergency Management (2021), floods caused by continuous precipitation in July 2020 affected 38.173 million people, and 3,868.7 thousand hectares of crops, and resulted in 109.74 billion yuan in direct economic losses; in August, 41.35 billion yuan in direct economic losses occurred.

In recent years, an increasing number of studies have linked increased precipitation extremes to human activities. Human activities have caused global changes in terrestrial precipitation (IPCC, 2021). By enhancing the water cycle, anthropogenic warming may influence mean and extreme precipitation (He and Soden, 2015; Li et al., 2021b; Tao et al., 2016; Vecchi et al., 2006; Wu et al., 2022). 2/3 of the land area of the Northern Hemisphere has experienced enhanced extreme precipitation, and multi-model simulations of precipitation response to anthropogenic forcing are consistent with changes in terrestrial extreme precipitation observed in the Northern Hemisphere (Min et al., 2011; Zhang et al., 2013). The more extreme the precipitation event, the clearer the anthropogenic influence (Wang et al., 2023). The human influence dominated by the GHG effect has intensified extreme precipitation, especially in continental and regional extreme precipitation (Chen and Sun, 2017; Dong et al., 2021; Kirchmeier-Young and Zhang, 2020; Sun et al., 2021; Xu et al., 2022). For the 2020 extreme precipitation, anthropogenic forcing has decreased the likelihood of the month-scale extreme rainfall that was observed in the lower Yangtze River in 2020 (Zhou et al., 2021; Lu et al., 2022;

Ma et al., 2022; Tang et al., 2022). However, the influence of anthropogenic forcing on RX1day over YZR, month-scale precipitation and RX1day over HHB regions in 2020 has received less attention.

Additionally, human activities may increase the probability of short-term heavy precipitation and decrease the frequency of long-term precipitation in China (Lu et al., 2020; Zhang et al., 2020). However, different studies defined events in different regions and the study areas are fragmented, leading to different conclusions (Stott et al., 2016). It has been suggested that human activities may have increased the risk of long-term persistent and short-term extreme precipitation in the Yangtze River basin and southern China (Sun and Miao, 2018; Sun et al., 2019; Yuan et al., 2018; Zhou et al., 2018). However, some scholars thought that human activities had reduced the risk of long-term precipitation in south of the Yangtze River and in southern China, increasing the risk of drought in early summer in Yunnan (Li et al., 2018; Li et al., 2021a; Lu et al., 2020; Nanding et al., 2020;). The reduced flood risks in west-central China may also be related to human activities (Ji et al., 2020; Zhang et al., 2020). Considering that the above studies involve different regions and time periods, it is difficult to make regional comparisons.

Greenhouse gases (GHG) and aerosols (AER) emissions are the two most important anthropogenic climate-forcing factors. Increases in GHG have contributed to the observed intensification of extreme precipitation over many land areas (Chen and Sun 2017; Dong et al. 2020, 2021; Lu et al. 2020), resulting from enhanced atmospheric water-holding capacity by GHG induced warming (Min et al. 2011; Zhang et al. 2013; Myhre et al., 2014; Lin et al. 2018;). AER can affect local climate directly by radiative absorption and scattering and indirectly by changing cloud characteristics like albedo and lifetime through their role as cloud condensation nuclei (Boucher et al. 2013; Bellouin et al., 2020). Some recent studies have demonstrated that increased AER emissions during the last few decades have played an important role in the observed weakening of the East Asian summer monsoon circulation (Polson et al., 2014; Dong et al. 2020; Song et al. 2014; Chen et al., 2018; Tian et al. 2018; Diao et al., 2021) and the reduced summer extreme precipitation over north China (Lin et al. 2018; Zhang et al. 2017; Guo et al. 2023). In addition to anthropogenic influences, strong natural variability is still nonnegligible in regulating regional precipitation extremes (Li et al., 2021a; Martel et al., 2018).

At the end of the 21st century, as global warming increases, the Asian monsoon region will become increasingly warm and wet, and sudden-onset floods such as urban rainfalls and flash floods, which are strongly associated with extreme precipitation, will become more frequent and severe (IPCC, 2021; Kharin et al., 2013; O'Gorman, 2012). GHG-induced warming will increase extreme precipitation significantly (Min et al., 2011; Myhre et al., 2014), while anthropogenic aerosol emission reductions will exacerbate extreme precipitation in East Asia (Lin et al., 2018; Myhre et al., 2014; Rotstayn et al., 2013; Wang et al., 2015; Xu et al., 2018; Zhao et al., 2019). The combination of the two could make extreme precipitation significantly more intense in the context of future warming. Thus, it is of great interest to quantify the risk of summer 2020-like extreme heavy precipitation events over China in future.

This paper analyzes heavy precipitation events in the summer 2020 in two regions over East China, namely the mid-lower reaches of the Yangtze River (YZR), the mid-lower reaches of the Yellow River- Hai River basin (HHB).

The main aims of the study are to assess the anthropogenic influences on the likelihood of heavy precipitation events in summer 2020 in two regions over East China using the Met Office HadGEM3-GA6 attribution system (Ciavarella et al. 2018) and the sixth phase of Coupled Model Inter-comparison Project (CMIP6) (Eyring et al. 2016; Gillett et al. 2016). In addition, the probability of summer 2020-like extreme precipitation events under different shared socioeconomic paths are projected and quantified.

The rest of the paper is organized as follows: in Section 2, observational and model data, as well as their analysis methods, are described. The simulated precipitation and precipitation extremes in summer over China are evaluated in Section 3. Section 4 focuses on the attribution of observed events, and Section 5 documents projected changes. The conclusion is given in Section 6.

2 DATA AND METHODS

2.1 Data

In this study, we used quality-controlled daily rainfall station data provided by the National Meteorological Information Center (NMIC) of China from over 2400 meteorological stations during 1961-2020. Cressman interpolation (Cressman, 1959) was used to interpolate the original station observations data to $0.56^{o} \times 0.83^{o}$ (the same as the HadGEM3-GA6 model resolution).

For the study period, atmospheric circulation conditions were analyzed using the global reanalysis dataset from the National Centers for Environmental Prediction (NCEP) and the National Center for the Atmosphere (NCAR) (Kalnay et al., 1996). The reanalysis data of the variables of geopotential height, temperature, precipitable water, sea level pressure, specific humidity, zonal and meridional winds were used, with a spatial resolution of $2.5^{o} \times 2.5^{o}$, a temporal resolution of days, and a vertical resolution of 17 layers for 3-dimension variables.

Based on the HadGEM3-GA6 model developed by Hadley Center (Ciavarella et al., 2018), with N216 resolution of 0.56° × 0.83°, this study examined the effects of anthropogenic forcings of 2020-like monthly-scale and daily extreme precipitation in two regions over East China. The model simulations include two sets of ensemble simulations. One set is ALL-forced (historical) simulations that are conditioned on observed sea surface temperatures (SST) and sea ice (HadISST) (Rayner et al., 2003). The other set is natural forced (historicalNat) simulations in which anthropogenic signals from observed SST are removed with preindustrial forcings. Both historical and historicalNat ensembles have 15 members in the historical period (1961-2013) and 525 members in 2020. Therefore, the occurrence probabilities and the resulting attribution conclusions are conditioned on the 2020 SST and sea ice.

To further validate the attribution conclusions, we used simulations from climate models that participated in the Coupled Model Intercomparison Project Phase 6 (CMIP6) and in Detection and Attribution Model Intercomparison Project (DAMIP) (Eyring et al. 2016; Gillett et al. 2016) under all anthropogenic and natural forcing combined (ALL), and natural forcing (NAT) with a set of 12 different climate models. Details of the models are given in Table 1 and Table S1. Since the coupled simulations have an evolving SST and sea ice, we chose the years 2011-2020, which are closest to 2020, using the SSP5-8.5 (Shared Socioeconomic Pathway 5/Representative Concentration Pathway 8.5, O'Neill, et al., 2016) to extend CMIP6 ALL simulations from 2014 to 2020, to represent the current climate. We consider all members in CMIP6 ALL and NAT simulations for the decade 2011-2020 as an ensemble. Taking month-scale precipitation over YZR as an example, there are 750 samples in the CMIP6 ALL ensemble (75 simulations multiplied by 10 years) and 570 samples in NAT ensembles, respectively. It is worth noting that, unlike the 2020 SST-based HadGEM3-GA6 model, the CMIP6 simulations cover a wide range of ocean states. Therefore, the event probabilities estimated below are differently conditioned, and the two datasets' attribution results will not be directly comparable.

In addition, simulations of the same set climate models (see Table S1) from the CMIP6 in the Scenario Model Comparison Program (ScenarioMIP, O'Neill, et al., 2016) were selected for the SSP2-4.5, SSP3-7.0, and SSP5-8.5 scenarios for 2081-2100 and these model simulations were used to assess the probability of the occurrence of summer 2020-like extreme precipitation events over China at the end of the 21st-century.

To reduce differences between models and observations, making the results more accurate, we perform a linear-scaling bias correction to the model simulations. Precipitation and RX1day are corrected with a factor based on the ratio of long-term monthly mean observed and simulated data during 1961-2010 (Teutschbein and Seibert, 2012).

For station data, we first calculated month-scale precipitation (or RX1day), and then calculated precipitation anomalies (or RX1day percentage anomalies) relative to 1961-2010 average at each station. To prevent errors in sparsely populated areas of stations, we used Cressman interpolation to interpolate RX1day and monthly precipitation station data to model resolution, and finally got the regional average of RX1day or monthly precipitation using area-weighted mean. For simulated data, we first calculated the indices at each grid on the original grid of each model then calculated the regional average to prevent errors during the interpolation process for simulated data. To remove model bias, monthly precipitation anomalies and RX1day percentage anomalies have been calculated using the 1961-2010 climatology. Details of the indices calculation process could be found in the Supplementary information.

TABLE 1 Overview of the 12 CMIP6 global climate models

CMIP6 Model	Country	CMIP6 Model	Country
ACCESS-CM2	Australia	IPSL-CM6A-LR	France
ACCESS-ESM1-5	Australia	MIROC6	Japan
BCC-CSM2-MR	China	CESM2	United States
CanESM5	Canada	FGOALS-g3	China
CNRM-CM6-1	France	MRI-ESM2-0	Japan
HadGEM3-GC31-LL	United Kingdom	NorESM2-LM	Norway

2.2 Methods

2.2.1 Selection of the study area

In summer (June-July-August) 2020, China had 14.7% more precipitation than normal, which is the second heaviest since 1961 (China Meteorological Administration, 2021). Flooding rainfall was mainly concentrated in the mid-lower reaches of the Yangtze River, with a 62-day-long plum rainy season and the heaviest plum rain since 1961. A total of 21 numbered floods occurred in major rivers such as the Yangtze, Yellow, and Huai Rivers (Ministry of Emergency Management, 2021). To investigate the contribution of anthropogenic impacts to extreme precipitation events in these regions over East China, respectively, this paper selects YZR and HHB regions where stations are densely distributed, as representative regions in south and north parts of the East China, respectively, for the summer 2020-like extreme precipitation events. The two study regions are shown in red boxes in Figure 1.

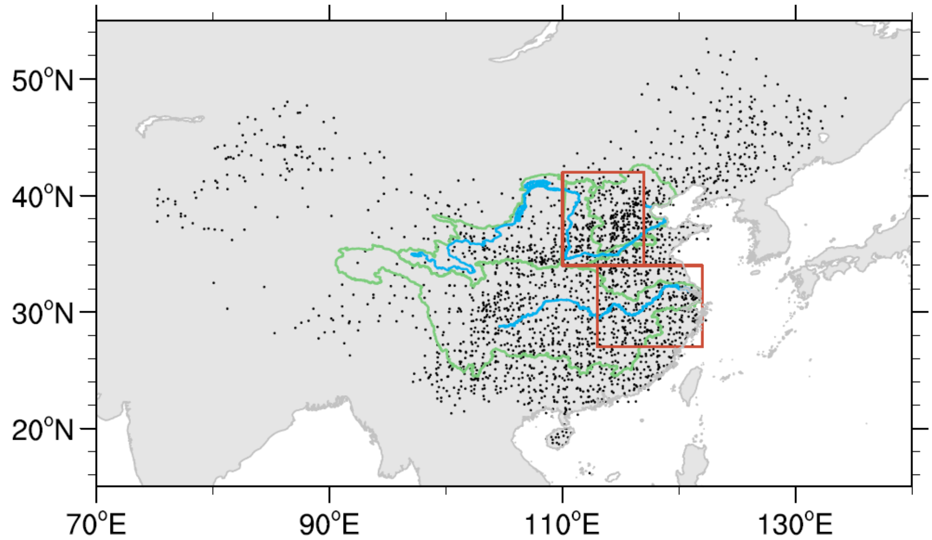

FIGURE 1 Study regions and distribution of weather stations used. Dots are stations of observations. Green lines highlight the Yangtze River basin, the Yellow River basin and Hai River basin. Red boxes highlight the study area of the mid-lower reaches of the Yangtze River (27~34^{o}N, 113~122^{o}E, YZR region), and the mid-lower reaches of the Yellow River- Hai River basin (34~42^{o}N, 110~117^{o}E, HHB region).

2.2.2 Observed precipitation extreme events in summer 2020 and event thresholds

Considering that the YZR and HHB are located in different latitudes and their peak precipitations usually occur at different times, we respectively focus on precipitation extreme events in different months for YZR and HHB.

The time evolution of daily summer precipitation over YZR in 2020 and the spatial distribution of precipitation anomalies in June-July are shown in Figure 2a~b. They show anomalous heavy precipitation in 2020 occurred in June-July over YZR, and therefore the attribution analysis in this study for YZR considers June-July month-scale precipitation and daily maximum precipitation (RX1day) during these two months. Details of calculating area averaged monthly precipitation and RX1day in a region are described in the Supplementary information. The regional averaged precipitation anomaly relative to the climate mean state in June-July 2020 is 5.2 mm/d and the regional averaged percentage change of RX1day relative to the climate mean is 40.4% (Figure 4 a, b), both of which were the highest since 1961. For the YZR region in the follow-up analysis, 5.2 mm/d and 40.4% were used as the threshold for the monthly extreme precipitation events and daily extreme precipitation in June-July for the attribution analysis respectively.

Figure 2c~d illustrates the time evolutions of daily summer precipitation in 2020 and the spatial distribution of precipitation anomalies in August. The attribution analysis will focus on extreme precipitation events in August 2020, which is a period accompanied by concentrated precipitation. As illustrated in Figure 4c the HHB regional averaged precipitation anomaly in August 2020 was 1.9 mm/d and the regional averaged RX1day percentage change was 39.6% above the corresponding climatology (Figure 4d), both of which were the third highest since 1961. Therefore, the monthly mean precipitation threshold of 1.9 mm/d and RX1day threshold of 39.6% in August were used in the attribution analysis for the HHB region. In summary, two precipitation indices based on observations in summer 2020 over the East China monsoon region were selected in this study for attribution analysis and future projection. They are June-July precipitation and RX1day over YZR and monthly precipitation and RX1day in August over HHB.

The atmospheric circulations in 2020 show that the South Asian high (SAH) extends eastward both in June-July and in August compared to the climatological position (Figure 3), and the Eastern Asian Subtropical Jet (EASJ) is stronger than normal, while the western Pacific subtropical high (WPSH) extends westward. The westward extension of WPSH leads to a large positive geopotential height anomaly and a strong southwest water vapor transport in June-July over YZR. As a result, heavy precipitation persists in the YZR region due to the convergence of warm and humid air from the south and cold air from the north. This study agrees with the findings of numerous studies that show high precipitation in the YZR region when WPSH is strong and its ridge extends southward and westward (Jin et al., 2018; Li et al., 2013; Tang et al. 2021; Nie et al., 2021).

Strong southwesterly and southerly winds can be found on the western and southern edges of the WPSH in August 2020, transporting water vapor from the Bay of Bengal and the western Pacific Ocean to the HHB region. Meanwhile, the northern hemisphere polar vortex is dipole-shaped and weaker than normal for the same period, and the Westerlies are strong. The high-pressure ridge is near Lake Balkhash. The HHB region is controlled by a weak trough over the east of Lake Baikal, so there are more weak cold air activities in the HHB region. Cold and warm air convergence causes more precipitation in the region than normal. This is consistent with the conclusion that the high precipitation in this region is closely related to the weak polar vortex, the anomalously strong westerlies in the upper troposphere, and the ridge of subtropical high being westward than normal in previous studies (e.g., Zhang et al, 2008; Zhou, 2009).

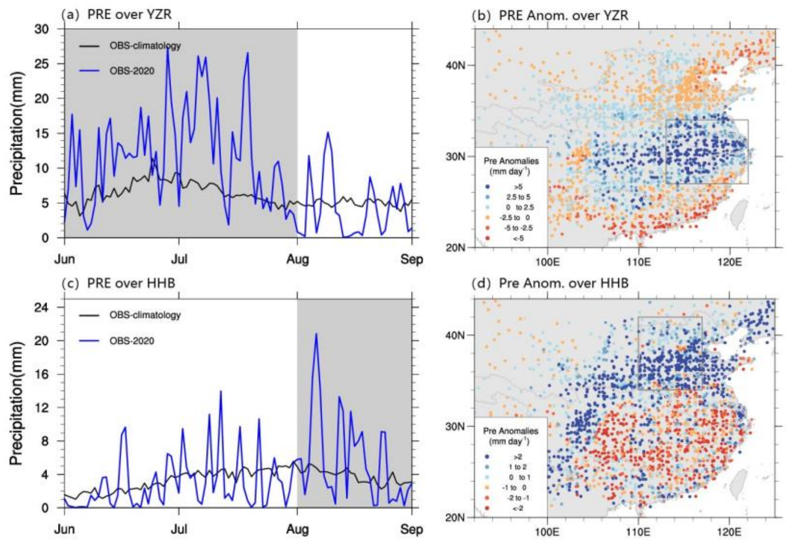

FIGURE 2 (a, c) Time series of observed daily precipitation (mm day^{-1}) for summer 2020 (blue) and climatology of 1961-2010 (black) for (a) YZR and (c) HHB. Grey shading indicates June-July and August respectively. (b, d) Spatial distributions of observed precipitation anomalies (mm day^{-1}) from rain gauges relative to 1961-2010 (b) in June-July over YZR and (d) in August over HHB. Black boxes in (b, d) highlight YZR and HHB regions.

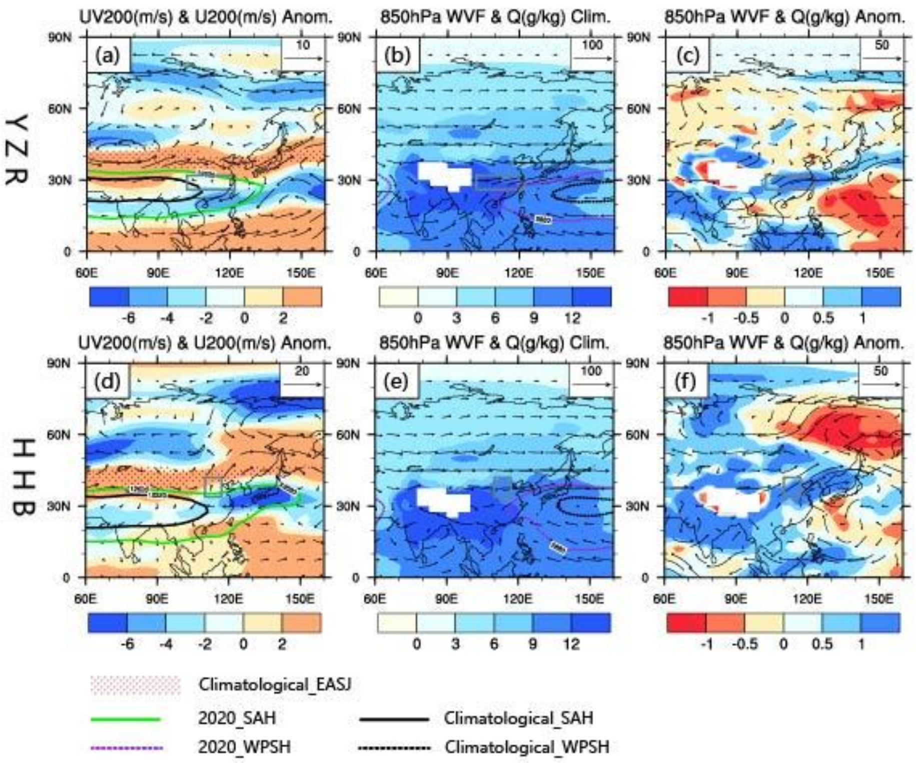

FIGURE 3 (a, d) Spatial distributions of 200-hPa wind vector (unit: m s^{-1}) and zonal wind (shaded, unit: m s^{-1}) anomalies relative to climatology 1961-2010. (b, c, e, f) Spatial distributions of water vapor flux (vector, unit: 1×10^{-6} kg hpa^{-1} m^{-1} s^{-1}) and specific humidity (shaded, unit: g kg^{-1}) at 850 hPa for (c, f) summer 2020 anomalies and (b, e) climatology of 1961-2010. The two rows show patterns in June-July (top panels) and in August (low panels). The solid green line represents the South Asian high (SAH) and the dashed purple line represents the Western Pacific subtropical high (WPSH), respectively. The black lines show their summer climatological positions. Red dotted areas represent the Eastern Asian Subtropical Jet (EASJ) (zonal wind speeds >24 m s^{-1} at 200hPa).

2.2.3 Attribution methods for extreme events

In the historical and historicalNat sets of HadGEM3-GA6 (or ALL and NAT in

CMIP6) simulations, the occurrence probability of precipitation events greater than or equal to the 2020 thresholds were identified as P_{ALL} and P_{NAT}, respectively. The risk ratios (RR) were calculated based on RR= P_{ALL} /P_{NAT} (National Academies of Sciences and Medicine, 2016). When RR>1, it means that human activities make the event more likely, and when RR<1, it means that human activities make the event less likely. We estimated the return period of 2020-like extreme events at the end of the 21st century by calculating the probability of precipitation events greater than or equal to the 2020 thresholds for different SSP scenarios which is defined as P_{FUT}.

In the uncertainty analysis, the RR uncertainty with a 90% confidence interval (CI) was estimated by identifying the empirical 5th and 95th percentile among 1,000 times resampling model ensemble members by using the Monte Carlo bootstrapping procedure (Christidis et al. 2013). With each bootstrap, model ensemble simulations are randomly resampled with replacement to obtain new data of the same length as the original. For CMIP6 simulations, we calculated the ensemble mean for each model first and then calculated the multimodel ensemble mean. For probability and RR estimation for indices, we took all members in the chosen period of selected models as a grand ensemble.

In previous studies, it has been shown that the monthly extreme precipitation anomalies in the East China follow a Gaussian distribution (Alam et al., 2018; Wang et al., 2019), whereas RX1day in East China is more consistent with the Generalized Extreme Value (GEV) distribution (Li et al, 2015; Papalexiou and Koutsoyiannis, 2013; Yang et al., 2013). However, RX1day in northern China follows a normal distribution (Wang et al., 2017). Therefore, in this study, for the month-scale cumulative precipitation over two regions, and RX1day over HHB, occurrence probability is estimated based on the Gaussian distribution and the probability of RX1day over YZR is based on the GEV distribution.

3 RESULTS AND DISCUSSIONS

3.1 Model evaluation on simulated precipitation and precipitation extremes during 1961-2010

Evaluation of HadGEM3-GA6 and CMIP6 simulations was carried out to determine whether these models could accurately reproduce the characteristics of precipitation and precipitation extremes in summer over the study regions in East China. Time series of observed precipitation anomalies, model simulated precipitation anomalies and model uncertainty, and corresponding probability density functions (PDFs) for monthly precipitation anomalies and RX1day anomalies are illustrated in Figure 4.

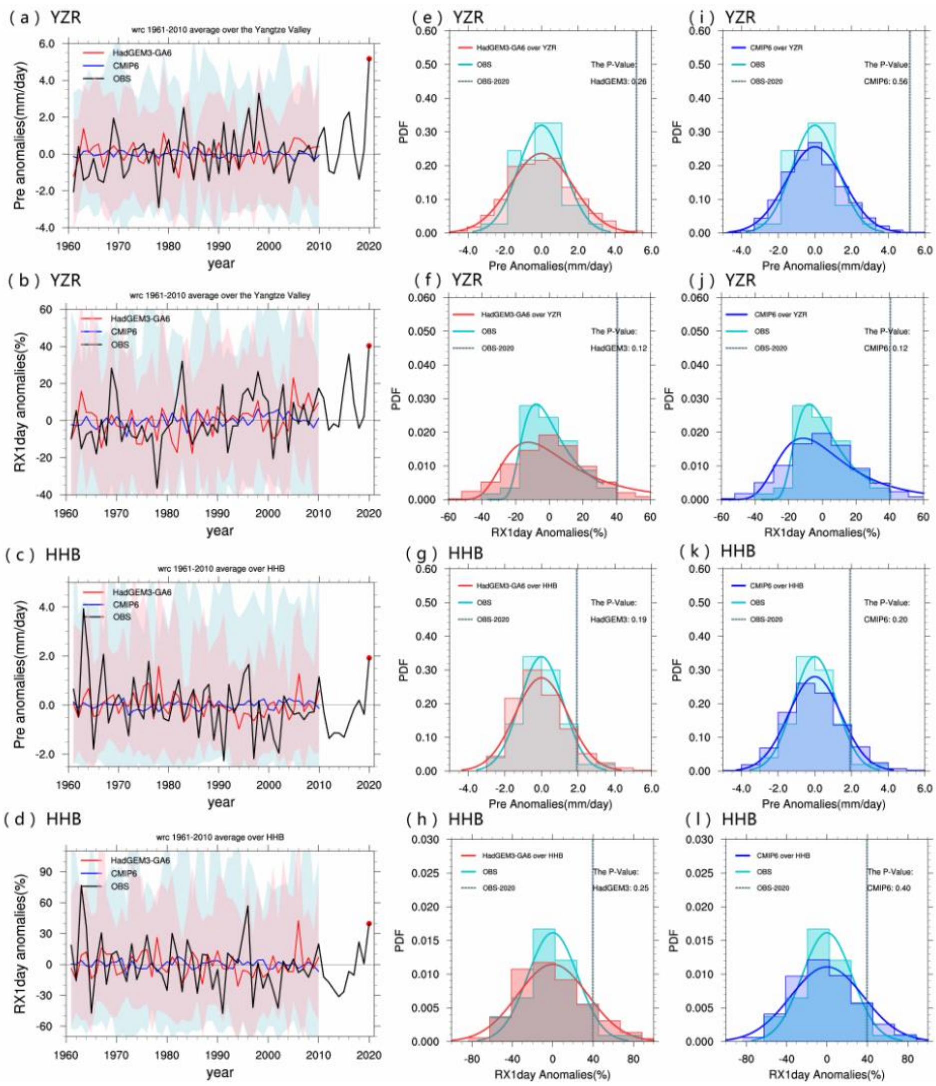

FIGURE 4 (a~d) Time series of anomalous precipitation (a, c, mm/day) and RX1day percentage anomalies (b, d, %) relative to the climatology of 1961-2010 in June-July over YZR and in August over HHB for observations and simulated ensemble means of OBS (black solid lines), HadGEM3 model (red solid lines) and CMIP6 multimodel mean (solid blue), and ensemble spreads of HadGEM3-GA6 (pink shading) and CMIP6 (blue shading), respectively. (e~l) PDFs of anomalous precipitation and RX1day percentage anomalies in June-July over YZR and in August over HHB respectively constructed using data from HadGEM3-GA6 historical experiments (red), CMIP6 historical experiments (blue) and OBS (green) from 1961 to 2010. The p-values based on the K-S test are given in each panel and vertical lines are corresponding values in 2020.

Results show that the observational anomalies were encompassed uncertainty ranges of model simulations (Figure 4 a-d). However, correlation coefficients between observational and the multi-ensemble mean time series (not shown) are low and these suggest that the interannual variability of monthly precipitation anomalies and RX1day anomalies in summer over East China is hard to well simulated considering the multi-scale feedback processes inherent in the Asian monsoon system. PDFs indicate that the distributions between HadGEM3-GA6 simulations and OBS precipitation indices anomalies in summer during 1961–2010 (Figure 4 e-l) cannot be distinguished at the 0.05 significance level based on the K-S test (with P-value being greater than 0.05), as well as CMIP6 simulations and OBS. The whole 12 CMIP6 models also passed the test individually (Table S2; Figure S1~S4) and details of model selection are documented in the Supplementary information. These model evaluations suggest that both HadGEM3-GA6 and CMIP6 models can be regarded as reliable for attributing monthly precipitation anomalies and RX1day anomalies in summer 2020 over East China.

3.2 Attribution of 2020-like extreme precipitation events in study regions

3.2.1 Events in YZR

To show the anthropogenic influences on the probability of precipitation extremes in summer 2020 over YZR, PDFs precipitation anomalies over YZR in June-July 2020 and RX1day percentage anomalies and corresponding return periods for these two indices in historical (ALL) and historicalNat (NAT) in HadGEM3-GA6 (CMIP6) model simulations are illustrated in Figure 5. One of the most important features in PDFs of monthly precipitation anomalies is a leftward shift in historical simulations relative to historicalNat and this suggests that historical (ALL) simulations tend to have less monthly precipitation than historicalNat (NAT) (Figure 5 a, b). HadGEM3-GA6 and CMIP6 simulations show consistent risk ratios of 0.41 [90% confidence intervals: 0.30, 0.47] and 0.53 [90% confidence intervals: 0.21, 1.31], respectively (Figure 6, Table 2). These results suggest that anthropogenic forcings significantly reduce the probability of the June-July extreme heavy precipitation event similar to 2020 in the YZR region by about 59% in HadGEM3 model and 47% in CMIP6 models. As shown in Figure 6, the best estimates of RR values in CMIP6 are all less than 1 except NorESM2-LM and FGOASLS-g3.

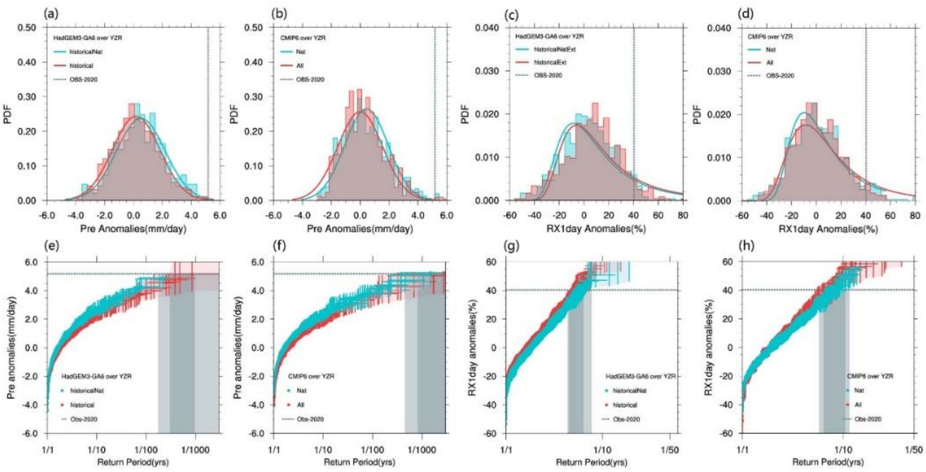

FIGURE 5 PDFs (a-d) and return periods (e-h) for June-July 2020 HadGEM3-GA6 and CMIP6 ALL (2011-2020) (red) and NAT (2011-2020) (green) simulated precipitation (a, b, e, f; mm/day) and RX1day percentage anomalies (c, d, g, h; %) in the YZR region. Each point in (e-h) represents an ensemble member with vertical and horizontal bars being the 5%-95% uncertainty interval of precipitation and RX1day percentage anomalies and return periods and grey and dark grey lines indicating the uncertainty interval of the return period of the threshold-exceedance in historical and historicalNat simulations, respectively. Vertical dotted lines in (a-d) and horizontal dotted lines in

(e-f) are corresponding values in 2020.

TABLE 2 Return periods and risk ratios of precipitation and RX1day percentage anomalies in June-July 2020 over the YZR region simulated by CMIP6 and HadGEM3 models and their uncertainty intervals (90% CI)

Index	**Models**		**Return Period (90% CI)**	**Risk ratios (90% CI)**
PRE	HadGEM3-GA6	historical	874.6(300.1, 3363.5)	0.41(0.30, 0.47)
		historicalNat	361.4(174.6, 969.7)	
	CMIP6	ALL	2271.2 (819.2, 9457.3)	0.53(0.21, 1.31)
		NAT	1223.9 (449.7, 5285.8)	
RX1day	HadGEM3-GA6	historical	5.4 (4.4, 6.3)	1.15 (1.04, 1.18)
		historicalNat	6.2 (4.5, 7.7)	
	CMIP6	ALL	7.2 (5.7, 10.4)	1.13(0.93, 1.41)
		NAT	8.4 (6.4, 11.5)	

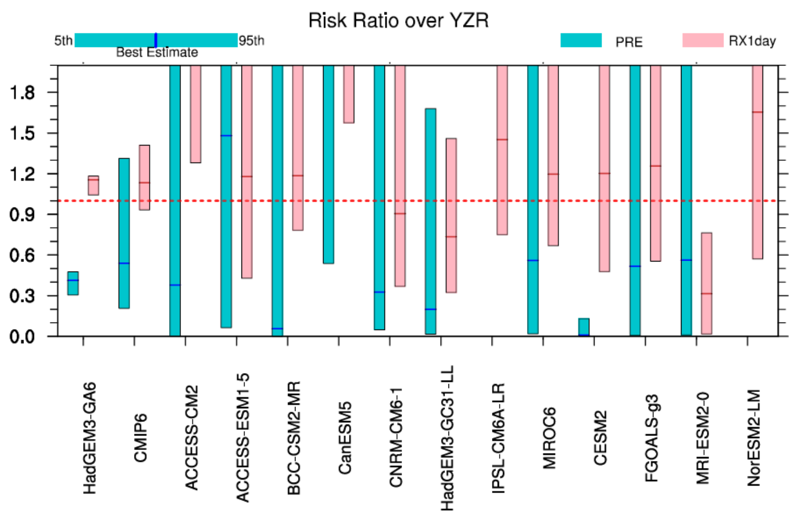

FIGURE 6 Risk ratios and their confidence intervals (90% CI) for the CMIP6 and HadGEM3-GA6 model simulating precipitation anomalies (green shading) and RX1day percentage anomalies (pink shading) in the YZR region. The solid lines indicate the best estimate of precipitation anomalies (green lines) and RX1day percentage anomalies (pink lines).

Variations in return periods are also indicative (Figure 5e, f) of anthropogenic effects reducing the likelihood of 2020-like June-July extreme precipitation events.

With only natural forcing, HadGEM3-GA6 shows a return period of 1 in 361 years, and with ALL forcing, it shows a return period of 1 in 875 years; CMIP6 model simulations show consistent changes in return period, and it changes from about 1 in 1224 years in NAT simulations to about 1 in 2271 years in ALL simulations. These attribution results suggest that human activities have reduced the probability of June-July 2020-like extreme precipitation events in the YZR region of East China, and this conclusion is robust for HadGEM3-GA6 and CMIP6 model simulations.

In contrast to the monthly precipitation in summer 2020, the analysis of RX1day shows that the probability of RX1day percentage anomalies larger or similar to June-July 2020 in historical (ALL) simulations are larger than historicalNat (NAT) (Figure 5c, d). The risk ratios (RR) estimated by HadGEM3-GA6 and CMIP6 are 1.15 [90% CI: 1.04, 1.18] and 1.13 [90% CI: 0.93, 1.41] (Figure 6, Table 2), implying that anthropogenic forcings increase the likelihood of summer 2020-like RX1day extreme heavy precipitation events by about 15% in YZR in HadGEM3-GA6 and 13% in CMIP6. However, there is some uncertainty in CMIP6 models with most models showing RR values greater than 1 except for CNRM-CM6-1, HadGEM3-GC3 1-LL, and MRI-ESM2-0. The variation of the return period (Figure 5g, h) indicates that the June-July 2020-like RX1day extreme precipitation events are more likely to occur due to anthropogenic influences. Based on HadGEM3-GA6 simulations, the return period is about 1 in 6.2 years with only natural forcing and about 1 in 5.4 with ALL forcing. CMIP6 model simulations show consistent changes in return period, and it changes from about 1 in 8.4 years in NAT simulations to about 1 in 7.2 years in ALL simulations.

3.2.2 Events in HHB

For 2020-like extreme precipitation events in representative HHB region of East China, the PDFs of month-scale precipitation and RX1day percentage anomalies in August show that anthropogenic forcings tend to increase the likelihood of both monthly-scale and RX1day extreme precipitation in HadGEM3-GA6 simulations, with the RR of 1.12 [90% CI: 1.11, 1.15] and 1.41 [90% CI: 1.37, 1.48] (Figure 7a, c, Figure 8, Table 3). The return periods gave consistent conclusions (Figure 7e, g, Table 3), with precipitation anomalies and RX1day return periods of 1 in 5.7 and 1 in 5.8 years under historicalNat simulations, while they changed to 1 in 5.1 and 1 in 4.1 years under historical simulations.

CMIP6 simulations show opposite results in monthly-scale extreme precipitation but are consistent in RX1day (Figure 7b, d). The PDF distribution curves for ALL simulations tend to shift left in comparison with those in NAT simulations, suggesting that anthropogenic forcings tend to reduce the likelihood of August-2020-like precipitation. Risk ratios (RR) are 0.77 [90% CI: 0.61, 0.94] (Figure 8, Table 3). Additionally, the return period demonstrates that the August 2020-like monthly precipitation extreme events are less likely to occur due to anthropogenic influences (Figure 7f, Table 3). Under the NAT simulation, the return period for monthly precipitation anomalies is 5.8 years, but under the ALL simulation is 7.5 years. Except for CNRM-CM6-1, CanESM5, and FGOALS-g3, most of CMIP6 models simulate RR values of precipitation anomalies that are less than 1 (Figure 8). The RR of RX1day estimated by CMIP6 is 1.02 [90% CI: 0.84, 1.27] (Figure 8, Table 3) which is not significant since the large spread among different models.

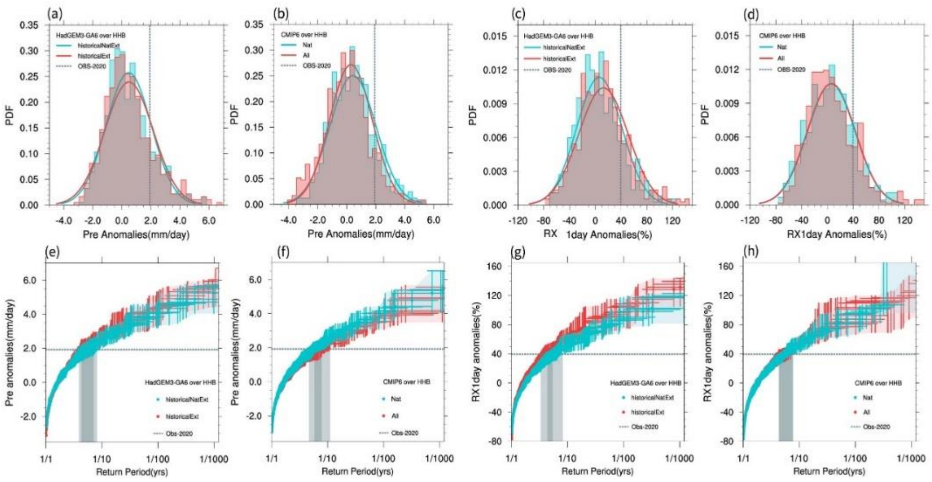

FIGURE 7 PDFs and return periods for August 2020 HadGEM3-GA6 and CMIP6 ALL (2011-2020)

and NAT (2011-2020) simulated precipitation (a, b, e, f; mm/day) and RX1day percentage anomalies (c, d, g, h; %) in the HHB region. Each point in (e-h) represents an ensemble member, with vertical and horizontal bars being the 5%-95% uncertainty interval of precipitation and RX1day percentage anomalies and return periods and grey and dark grey lines indicating the uncertainty interval of return period of the threshold-exceedance in historical and historicalNat simulations, respectively. Vertical dotted lines in (a-d) and horizontal dotted lines in (e-f) are corresponding values in 2020.

TABLE 3 Return periods and risk ratios of precipitation and RX1day percentage anomalies in August 2020 in the HHB region simulated by CMIP6 and HadGEM3-GA6 models and their uncertainty intervals (90% CI)

Index	Models		Return Period (90% CI)	Risk ratios (90% CI)
PRE	HadGEM3-GA6	historical	5.1 (3.9, 7.1)	1.12 (1.11, 1.15)
		historicalNat	5.7 (4.3, 8.2)	
	CMIP6	ALL	7.5 (5.8, 11.1)	0.77 (0.61, 0.94)
		NAT	5.8 (4.7, 7.8)	
RX1day	HadGEM3-GA6	historical	4.1 (3.3, 5.4)	1.41 (1.37, 1.48)
		historicalNat	5.8 (4.4, 8.0)	
	CMIP6	ALL	5.4 (4.3, 7.7)	1.02 (0.84, 1.27)
		NAT	5.5 (4.4, 7.8)	

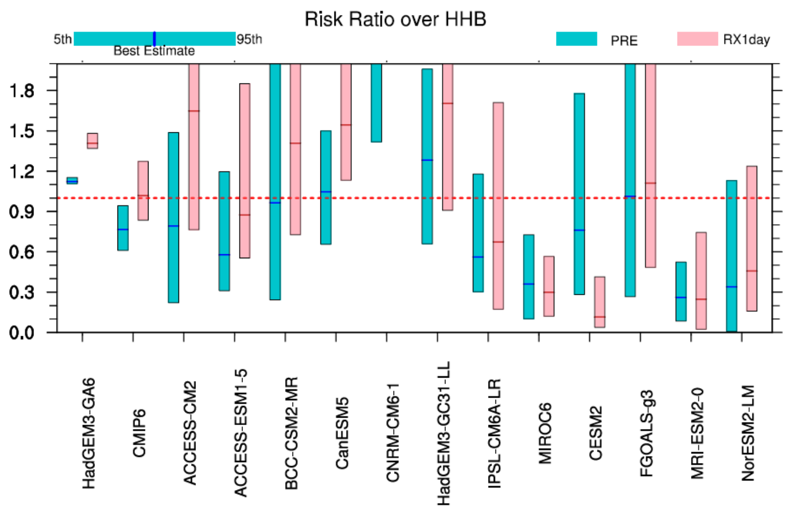

FIGURE 8 Risk ratios and their uncertainty intervals (90% CI) for the CMIP6 and HadGEM3

models simulating precipitation anomalies (green shading) and RX1day percentage anomalies (pink shading) in the HHB region. The solid lines indicate the best estimate of precipitation anomalies (green lines) and RX1day percentage anomalies (pink lines).

3.2.3 Difference between the two attribution systems

The main attribution results based on two attribution systems in two regions of East China are summarized in Table 4. These results show consistent conclusions for June-July precipitation extremes and RX1day in 2020 over the YZR region between CMIP6 and HadGEM3-GA6 model simulations. However, attribution results are inconsistent in the HHB region between the two models, especially for August monthly precipitation in 2020. HadGEM3-GA6 simulations show an increase of likelihood by 12% while CMIP6 models show a decrease of 23% based on anthropogenic forcing. The reasons responsible for these contrasting results between two different systems need to be investigated further. These contrasting attribution results suggest that one has to draw the attribution conclusion carefully and multiple methods might need to make helpful attribution conclusions in this region.

Spatial patterns of multimodel mean (ensemble mean for HadGEM3-GA6) changes in June-July and August precipitation in response to anthropogenic forcings among two systems over East China are illustrated in Figure 9. In June-July, two models show common features of reduced precipitation in YZR, which is consistent with reduced likelihood of extreme monthly precipitation in this region. However, there are some different spatial distributions of precipitation anomalies. The main feature in CMIP6 models is a dipole pattern of precipitation anomalies with reduced precipitation over YZR and increased precipitation HHB. In contrast, HadGEM3-GA6 shows reduced precipitation in both regions.

In August, CMIP6 models show a dipole pattern with reduced precipitation over the HHB region and increased precipitation to the south while HadGEM3-GA6 shows an opposite dipole with increased precipitation in HHB and reduced precipitation over large parts of southern China. These different spatial distributions of multimodel mean monthly precipitation over East China in response to anthropogenic forcing can explain different attribution results in the HHB region between two models.

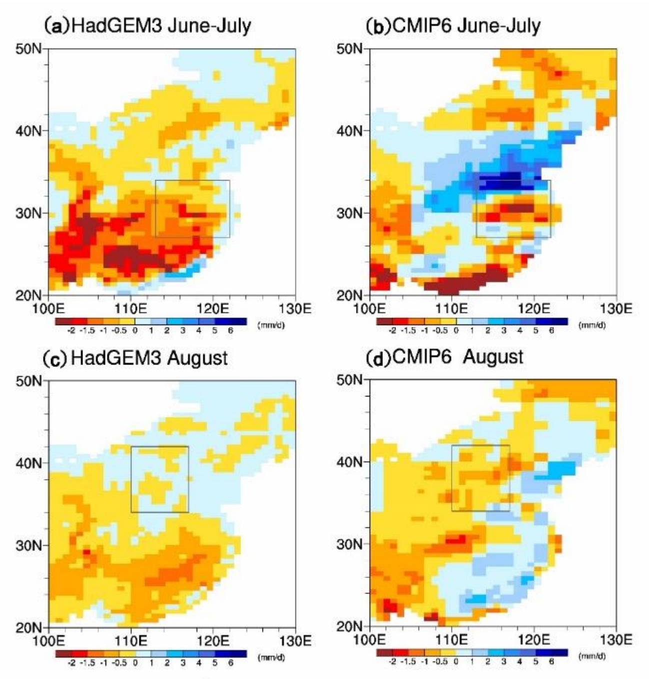

FIGURE 9 Spatial distributions of precipitation difference (mm day^{-1}) between with and without anthropogenic forcing by using HadGEM3 (a, d) and CMIP6 (b, d) models in June-July (a, b) and in August (c, d). Black boxes in (a, b) and (c-d) highlight YZR and HHB regions.

TABLE 4 The human influence on Pre and Rx1day for YZR and HHB

		YZR Month-scale Pre	YZR Rx1day	HHB Month-scale Pre	HHB Rx1day
Human influence	CMIP6	Decrease	Increase	Decrease	Increase
	HadGEM3	Decrease	Increase	Increase	Increase
Risk Ratio	CMIP6	0.53 (0.21,1.31)	1.13 (0.93, 1.41)	0.77 (0.61, 0.94)	1.02 (0.84, 1.27)
	HadGEM3	0.41 (0.30,0.47)	1.15 (1.04, 1.18)	1.12 (1.11,1.15)	1.41 (1.37, 1.48)

CMIP6 models are fully coupled models and HadGEM3-GA6 is an atmospheric only model. Why two models show some different features in seasonal evolutions of precipitation in response to anthropogenic forcing? This is an important question. Previous studies showed that anthropogenic forcings affect regional precipitation through both thermodynamical contributions related to change in humidity in the atmosphere and dynamical contributions related to changes in atmospheric circulation (e.g., Tian et al 2018, Guo et al. 2023, Li et al. 2022). Thermodynamical contributions showed less spatial variations while dynamical contributions show large spatial variations related to changes in atmospheric circulation (e.g., Tian et al. 2018, Guo et al. 2023, Li et al. 2022). It would be valuable to investigate atmospheric circulation and thermal variable response to anthropogenic forcing in CMIP6 models and HadGEM3-GA6 model to understand regional precipitation changes. However, to address this is beyond the scope of this study.

3.2.4 Contributions from different forcing factors of human activities

Based on the attribution analysis above, it is suggested that anthropogenic forcings have contributed to the occurrence of extreme precipitation events similar to those in the summer 2020 in two regions over East China. As the two most important anthropogenic forcing factors, what are the respective contributions of GHG and AER to the changes in the likelihood of precipitation events? To answer this question, the DAMIP simulations of the historical, historicalNat, historicalAER, and historicalGHG experiments were used to quantify the contributions of GHG and AER on the likelihood of June-July and August precipitation and RX1day percentage anomalies in summer 2020 in the YZR and HHB regions.

PDFs and return periods due to different forcings are shown in Figure 10 and Table 5. Results indicate that anthropogenic aerosol emissions have reduced the likelihood of 2020-like month-scale precipitation and corresponding RX1day extreme events in June-July over YZR and August over HHB. These changes correspond to increases in return period for YZR and HHB precipitation events and RX1day in both regions. The greenhouse gas emissions from human activities increase the likelihood of both events, leading to decreases of return period for summer 2020-like events. As the influences of aerosol emissions are stronger than those of changes in GHG, human activities have reduced the likelihood of the monthly extreme precipitation over both YZR and HHB.

TABLE 5 Return periods and their uncertainty intervals (90% CI) for precipitation and RX1day percentage anomalies in June-July over YZR and in August over HHB simulated by CMIP6 under different forcing factors.

Region	**Models**		**PRE Return Period (90% CI)**	**RX1day Return Period (90% CI)**
YZR	CMIP6	ALL	2271.2 (819.2, 9457.3)	7.2 (5.7, 10.4)
		NAT	1223.9 (449.7, 5285.8)	8.4 (6.4, 11.5)
		AER	18682.9 (4487.1, 174762.7)	11.2 (7.8, 15.7)
		GHG	201.0 (101.6, 606.9)	4.9 (3.9, 6.2)
HHB	CMIP6	ALL	7.5 (5.8, 11.1)	5.4 (4.3, 7.7)
		NAT	5.8 (4.7, 7.8)	5.5 (4.4, 7.8)
		AER	14.1 (8.7, 27.3)	11.2 (7.3, 20.9)
		GHG	3.9 (3.2, 5.2)	3.5 (2.9, 4.5)

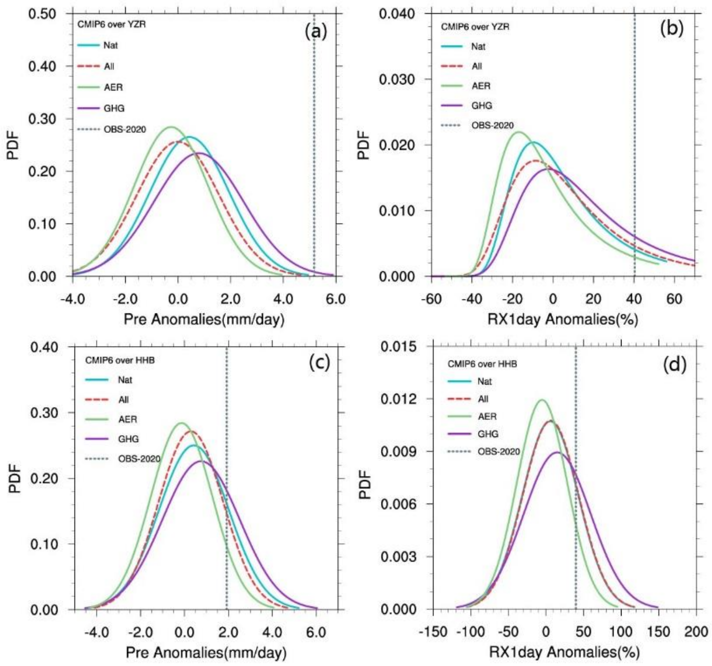

FIGURE 10 PDFs of CMIP6 simulated 2020-like extreme precipitation and RX1day events for (a, c) YZR regions in June-July and (b, d) HHB in August and under different factors of human forcing. Vertical dotted lines are corresponding values in 2020.

The above conclusion is consistent with the results by Tian (2018) that increasing GHG leads to increased precipitation by increasing the moisture transport convergence over eastern China, while aerosol forcing leads to divergent wind anomalies over northern China and reduced precipitation by weakening the EASM. In contrast, GHG induced increase of the probability of RX1day similar to the 2020 events in both regions is larger than AER induced decrease, leading to an increase of the probability of RX1day similar to the 2020 events although the increased probability is not significant due to large spread among different models in the HHB region.

3.3 Projected changes in the likelihood of similar extreme precipitation events in summer 2020 at the end of the 21st century

As greenhouse gas emissions will increase and anthropogenic aerosol emissions will decrease at the end of the 21st century, how will the probability of 2020-like extreme precipitation events happening over China by changing with global warming? To address this question, the CMIP6 simulations under scenarios SSP2-4.5, SSP3-7.0, and SSP5-8.5 were analyzed, and results on return periods are shown in Figure 11 and Table 6. One of the most important features is the decrease of return periods for monthly precipitation anomalies and RX1day percentage anomalies, although the magnitude of decrease depends on the scenarios. The largest change is anticipated for heavy precipitation over YZR in June–July 2020. and the return period for this kind of extremely rare event changes from 1 in 2271.2 years in present-day climate to 1 in 202.8/76.2/36.4 yearly events at the end of the 21st century under different scenarios. The above indicates an increase of the likelihood of this kind of event by more than 10 times.

The return period of 2020-like RX1day extreme precipitation events similar to that occurred over YZR changes from 1 in 7.2 years to 1 in 4.6/3.2/2.6 yearly events, suggesting this kind of event would be about doubled at the end of the 21st century. Under all three scenarios, return periods of heavy precipitation events that occurred in

August 2020 over the HHB region are shortened from 1 in 7.5 years in present day climate to 1 in 3.4/3.2/2.8 years at the end of the 21st century, and RX1day is shortened from 1 in 5.4 years to 1 in 2.9/2.8/2.3 years, suggesting that August 2020-like heavy precipitation events over the HHB region would become more frequent.

TABLE 6 Return periods and their confidence interval (90% CI) for 2020-like extreme precipitation and RX1day percentage anomalies in June-July over YZR and August over HHB simulated by CMIP6 for different future scenarios at the end of the 21st century.

Region	**Models**		**PRE Return Period (90% CI)**	**RX1day Return Period (90% CI)**
YZR	CMIP6	ALL-2020	2271.2 (819.2, 9457.3)	7.2 (5.7, 10.4)
		SSP2-4.5	202.8 (99.6, 532.4)	4.6 (3.8, 5.4)
		SSP3-7.0	76.2 (41.6, 185.5)	3.2 (2.8, 3.7)
		SSP5-8.5	36.4 (24.9, 74.2)	2.6 (2.3, 2.9)
HHB	CMIP6	ALL-2020	7.5 (5.8, 11.1)	5.4 (4.3, 7.7)
		SSP2-4.5	3.4 (2.9, 4.4)	2.9 (2.5, 3.6)
		SSP3-7.0	3.2 (2.8, 4.1)	2.8 (2.4,3.3)
		SSP5-8.5	2.8 (2.4, 3.4)	2.3 (2.1, 2.7)

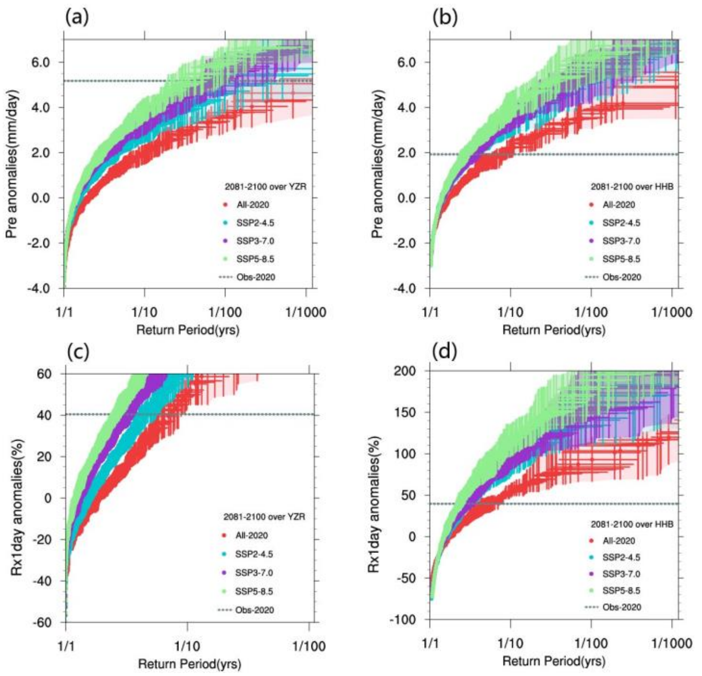

FIGURE 11 Return period and its uncertainty interval for 2020-like extreme precipitation anomalies

(a, b) and RX1day percentage anomalies (c, d) and their comparisons. (a, c) for June-July in the YZR region, (b, d) for August in the HHB region. Each point in (a-d) represents an ensemble member with vertical and horizontal bars being the 5%-95% uncertainty interval of precipitation and RX1day percentage anomalies and return periods. Horizontal dotted lines in (a-d) are corresponding values in 2020.

4 CONCLUSIONS

Historical simulation experiments using HadGEM3-GA6 and CMIP6 models with and without anthropogenic influence were conducted to attribute extremely heavy precipitation events in summer of 2020 over East China. We focus on a comparative study of the attribution results of monthly extreme precipitation and daily extreme precipitation in the mid-lower reaches of the Yangtze River basin as the representative south region and the lower reaches of the Yellow River- Hai River basin as the representative north region of the East China monsoon region. The main conclusions are as follows.

(1) For month-scale extreme precipitation events in the south of the East China monsoon region, human activities have reduced the likelihood of occurrence of this kind event. In other words, the occurrence of such extreme precipitation events is largely dependent on natural variability. For RX1day extreme precipitation events, anthropogenic factors have increased their probability both in north and south of the East China monsoon region. However, attribution results for August monthly precipitation in 2020 are inconsistent in the HHB region between two models, related to different spatial distributions of CMIP6 multi-model mean (HadGEM3-GA6 multi-ensemble mean) monthly precipitation over East China in response to anthropogenic forcing.

Our result is consistent with those of previous studies that human influence may have a dramatic impact on extreme precipitations (Min et al., 2011; Kirchmeier-Young et al., 2020; Paik et al., 2020). While Natural variability will dominate interannual variations in seasonal extreme precipitation in regional scales over the climate change signal (Martel et al., 2018; Li et al., 2021a). For 2020 extreme precipitation, anthropogenic forcing has decreased the likelihood of the month-scale extreme rainfall that was observed in the lower Yangtze River in 2020 (Zhou et al., 2021; Lu et al., 2022; Ma et al., 2022; Tang et al., 2022).

(2) In terms of different factors of human activities, anthropogenic aerosol forcing reduces both 2020-like monthly extreme precipitation and RX1day events; greenhouse gases increase the likelihood of both. As the influences of anthropogenic aerosol emissions are stronger than those of changes in GHG on monthly precipitation, human activities have reduced the likelihood of the monthly extreme precipitation over both YZR and HHB in CMIP6 model simulations. In contrast, GHG induced increase of the probability of RX1day similar to the 2020 events in both regions is larger than AER induced decrease, leading to an increase of the probability of RX1day similar to the 2020 events.

Our findings support the widely held belief that increased aerosol forcing reduces the severity of precipitation in China's eastern monsoon region (Zhao et al., 2006; Zhang et al., 2020). This is also consistent with a recent study by Yang et al. (2022) who found that the reduction of aerosol emissions during the COVID-19 pandemic led to abnormal land warming in eastern China, which enhanced the atmospheric circulation between eastern China, the South China Sea and the Philippine Sea, causing water vapor to be transported to China, ultimately leading to increased precipitation in Eastern China.

(3) Both the monthly extreme precipitation and RX1day events will become more frequent and the recurrence periods will shorten in both study regions by the end of the 21^{st} century. High emission scenarios show a greater increase in likelihood and a decrease in return period, which indicates that extreme precipitation risk increases with the concentration of greenhouse gases. Given the devastating impacts of these precipitation extreme events, our results suggest people will encounter much fiercer

changes of precipitation and precipitation extreme over China in the future and China would face a challenge to take adaptation measures to cope with those projected changes. Urgent actions need to be taken to control greenhouse gases emissions to avoid worse-case scenarios and to limit the damages from the increased risk of extreme heavy precipitation events. Carbon peaking and carbon neutrality should be realized as early as possible by policymakers through implementing sustainable development strategies and optimizing the energy structure.

AUTHOR CONTRIBUTIONS

Rouke Li: Conceptualization; methodology; investigation; visualization; writing – original draft; writing – review and editing. Xiaodong Liu: Conceptualization; writing – review and editing; funding acquisition. Ying Xu: Software, writing – review & editing, funding acquisition. Buwen Dong: Supervision; methodology; writing – review and editing.

ACKNOWLEDGEMENTS

We thank two anonymous reviewers and editor for their constructive comments and suggestions, which strengthened the manuscript considerably. This work is supported by the National Natural Science Foundation of China (41991254) and China Three Gorges Corporation (0704081), and the key Youth Innovation Team of China Meteorological Administration (CMA2023QN15). We thank the team of model developers and infrastructure experts for conducting the large HadGEM3-GA6 simulation campaign, and the Climate Science for Service Partnership (CSSP)-China programme for providing data access. We acknowledge the World Climate Research Programme's Working Group on Coupled Modelling and the individual modelling groups for their roles in making CMIP6 data available.

ORCID

Rouke Li. https://orcid.org/0000-0002-9774-9370

Xiaodong Liu. https://orcid.org/0000-0003-0355-5610

Buwen Dong. https://orcid.org/0000-0003-0809-7911

REFRENCES

Alam, M.A., Farnham, C. & Emura, K. (2018) Best-fit probability models for maximum monthly rainfall in bangladesh using gaussian mixture. *Geosciences*, **8**(4), 138. Available from: https://doi.org/10.3390/geosciences8040138

Bellouin, N., Quaas, J., Gryspeerdt, E., Kinne, S., Stier, P., Watson-Parris, D. et al. (2020). Bounding global aerosol radiative forcing of climate change. *Reviews of Geophysics*, **58**, e2019RG000660. Available from: https://doi.org/10.1029/2019RG000660

Boucher, O., Randall, D., Artaxo, P., Bretherton, C., Feingold, G., Forster, P. et al. (2013) *Clouds and aerosols. In Climate Change 2013: The Physical Science Basis. Contribution of Working Group I to the Fifth Assessment Report of the Intergovernmental Panel on Climate Change.* Cambridge University Press, DOI:10.1017/CBO9781107415324.016

China Ministry of Emergency Management. (2021). *National Natural Disaster Fundamentals 2020*, accessed 08 Janurary 2021, Available from: https://www.mem.gov.cn/xw/yjglbgzdt/202101/t20210108_376745.shtml

China Meteorological Administration. (2021). *China Climate Bulletin 2020*, Beijing: China Meteorological Press.

China Meteorological Administration (2022) *Blue Book on Climate Change in China 2021*, Beijing: Science Press.

Chen, G., Wang, W.C. & Chen, J.P. (2018) Circulatory responses to regional aerosol climate forcing in summer over East Asia. *Climate Dynamics*, **51**(11), 3973-3984. Available from: https://doi.org/10.1002/joc.6887

Chen, H.P. & Sun, J.Q. (2017) Contribution of human influence to increased daily precipitation extremes over China. *Geophysical Research Letters*, **44**, 2436-2444. Available from:

https://doi.org/10.1002/2016GL072439

Christidis, N., Stott, P.A., Scaife, A.A., Arribas, A., Jones, G.S., Copsey, D. et al. (2013) A New HadGEM3-A-Based System for Attribution of Weather- and Climate-Related Extreme Events. *Journal of Climate*, **26**, 2756-2783. Available from: https://doi.org/10.1175/JCLI-D-12-00169.1.

Ciavarella, A., Christidis, N., Andrews, M., Groenendijk, M., Rostron, J., Elkington, M. et al. (2018) Upgrade of the HadGEM3-A based attribution system to high resolution and a new validation framework for probabilistic event. *Weather and Climate Extremes*, **20**, 9-32. Available from: https://doi.org/10.1016/j.wace.2018.03.003.

Cressman, G. P. (1959) An Operational Objective Analysis System. *Monthly Weather Review*, **87**, 367–374. Available from: https://doi.org/10.1175/1520-0493(1959)087<0367:AOOAS>2.0.CO;2

Diao, C., Xu, Y. & Xie, S.P. (2021) Anthropogenic aerosol effects on tropospheric circulation and sea surface temperature (1980-2020): Separating the role of zonally asymmetric forcings. *Atmosphere Chemical and Physics*, **21**(24), 18499-18518. Available from: https://doi.org/10.5194/acp-21-18499-2021

Dong, S.Y., Sun, Y. & Li, C. (2020) Detection of human influence on precipitation extremes in Asia. *Journal of Climate*, **33**, 5293–5304. Available from: https://doi.org/10.1175/JCLI-D-19-0371.1.

Dong, S.Y., Sun, Y., Li, C., Zhang, X.B., Min, S. & Kim, Y. (2021) Attribution of extreme precipitation with updated observations and CMIP6 simulations. *Journal of Climate*, **34**(3), 871–881. Available from: https://doi.org/10.1175/jcli-d-19-1017.1

Eyring, V., Bony, S., Meehl, G. A., Senior, C. A., Stevens, B., Stouffer, R. J. et al. (2016) Overview of the coupled model intercomparison project phase 6 (CMIP6) experimental design and organization. *Geoscientific Model Development*. **9**, 1937–1958. Available from: https://doi.org/10.5194/gmd-9-1937-2016

Gillett, N. P., Shiogama, H., Funke, B., Hegerl, G., Knutti, R., Matthes, K. et al. (2016) The Detection and Attribution Model Intercomparison Project (DAMIP v1.0) contribution to CMIP6. *Geoscientific Model Development*, **9**, 3685-3697. Available from: https://doi.org/10.5194/gmd-9-3685-2016

Guo, Y., Dong, B.W. & Zhu, J.S. (2023) Anthropogenic impacts on changes in summer extreme precipitation over China during 1961–2014: roles of greenhouse gases and anthropogenic aerosols.

Climate Dynamic, **60**, 2633–2643. Available from: https://doi.org/10.1007/s00382-022-06453-4

He, J. & Soden, B.J. (2015) Anthropogenic Weakening of the Tropical Circulation: The Relative Roles of Direct CO_2 Forcing and Sea Surface Temperature. *Journal of Climate*, **28**(22), 8728-8742. Available from: https://doi.org/https://doi.org/10.1175/JCLI-D-15-0205.1

IPCC. (2021) *Climate Change 2021: The Physical Science Basis. Contribution of Working Group I to the Sixth Assessment Report of the Intergovernmental Panel on Climate Change of the United States of America*. Cambridge University Press, Cambridge, United Kingdom and New York, NY, USA. DOI:10.1017/9781009157896.

Ji, P., Yuan, X., Jiao, Y., Wang, C., Han, S. & Shi, C. (2020) Anthropogenic Contributions to the 2018 Extreme Flooding over the Upper Yellow River Basin in China. *Bulletin of the American Meteorological Society*, **101**(1), S89-S94. Available from: https://doi.org/10.1175/BAMS-D-19-0105.1

Jin, A.H., Zeng, G., YU, Y., Deng, W.T. & Li, Z.X. (2018) Influence of the meridional and latitudinal position configuration of South Asian high pressure and western Pacific subtropical high on summer precipitation in eastern China (in Chinese). *Journal of Tropical Meteorology*, **34**(6), 806-818. Available from: https://doi.org/10.16032/j.issn.1004-4965.2018.06.009

Kalnay, E., Kanamitsu, M., Kistler, R., Collins, W., Deaven, D., Gandin, L. et al. (1996) The NCEP/NCAR 40-Year Reanalysis Project. *Bulletin of the American Meteorological Society*, **77**(3), 437-472. Available from: https://doi.org/10.1175/1520-0477(1996)077<0437:TNYRP>2.0.CO;2

Kharin, V.V., Zwiers, F.W., Zhang, X.B. & Wehner, M.F. (2013) Changes in Temperature and Precipitation Extremes in the CMIP5 Ensemble. *Climatic Change*. **119**, 345-357. Available from: https://doi.org/10.1007/s10584-013-0705-8.

Kirchmeier-Young, M.C. & Zhang, X. (2020) Human influence has intensified extreme precipitation in North America. *Proceedings of the National Academy of Sciences*, **117**, 13308-13313. Available from: https://doi.org/10.1073/pnas.1921628117

Li, C., Tian, Q., Yu, R., Zhou, B., Xia, J., Burke, C. et al. (2018) Attribution of extreme precipitation in the lower reaches of Yangtze River during May 2016. *Environmental Research Letters*. **13**(1), 014015. Available from: https://doi.org/10.1088/1748-9326/aa9691.

Li, H., Zhou, S.W. & Wang, Y.F. (2013) A review on the relationship between subtropical high anomalies over West Pacific and summer precipitation in the middle-lower reaches of the Yangtze River(in Chinese). *Journal of Meteorology and Environment*, **29**(1), 93-102. Available from: https://doi.org/10.3969/j.issn.1673-503X.2013.01.016

Li, R.K., Li, D.L., Nanding, N., Wang, X., Fan, X.W., Chen, Y. et al. (2021a) Anthropogenic influences on heavy precipitation during the 2019 extremely wet rainy season in Southern China. *Bulletin of the American Meteorological Society*. **102**(1), S103-S109. Available from: https://doi.org/10.1175/BAMS-D-20-0135.1.

Li, T., Wang, Y., Wang, B., Ting, M., Ding, Y., Sun, Y. et al. (2022) Distinctive South and East Asian Monsoon circulation responses to global warming. *Science Bulletin*, **67**(7), 762-770. Available from: https://doi.org/10.1016/j.scib.2021.12.001.

Li, W., Chen, Y. & Chen, W. (2021b) The emergence of anthropogenic signals in mean and extreme precipitation trends over China by using two large ensembles. *Environmental Research Letters*, **16**(1), 014052. Available from: https://doi.org/10.1088/1748-9326/abd26d

Li, Z., Li, Z., Zhao, W. & Wang, Y. (2015) Probability Modeling of Precipitation Extremes over Two River Basins in Northwest of China. *Advances in Meteorology*, **2015**(6), 1-13. Available from: https://doi.org/10.1155/2015/374127

Lin, L., Gettelman, A., Fu, Q. & Xu, Y. (2018) simulated differences in 21st-century aridity due to different scenarios of greenhouse gases and aerosols. *Climatic Change*, **146**(3), 407-422. Available from: https://doi.org/10.1007/s10584-016-1615-3

Lu, C., Chen, R., Jiang, J. & Ullah, S. (2020) Anthropogenic influence on 2019 persistent drought in southwestern China. *Bulletin of the American Meteorological Society*, **101**(1), S65-S70. Available from: https://doi.org/10.1175/BAMS-D-20-0128.1

Lu, C., Sun, Y. & Zhang, X. (2022) The 2020 Record-Breaking Mei-yu in the Yangtze River Valley of China: The Role of Anthropogenic Forcing and Atmospheric Circulation. *Bulletin of the American Meteorological Society*, **103**, S98–S104. Available from: https://doi.org/10.1175/BAMS-D-21-0161.1.

Ma, Y., Z. Hu, X. Meng, F. Liu & W. Dong (2022) Was the Record-Breaking Mei-yu of 2020 Enhanced by Regional Climate Change? *Bulletin of the American Meteorological Society*, **103**, S76–S82. Available from: https://doi.org/10.1175/BAMS-D-21-0187.1.

Martel, J.L., Mailhot, A., Brissette, F. & Caya, D. (2018) Role of Natural Climate Variability in the Detection of Anthropogenic Climate Change Signal for Mean and Extreme Precipitation at Local and Regional Scales. *Journal of Climate,* **31**(11), 4241-4263. Available from: https://doi.org/10.1175/JCLI-D-17-0282.1

Min, S.K., Zhang, X., Zwiers, F.W. & Hegerl, G.C. (2011) Human contribution to more-intense precipitation extremes. *Nature,* **470**(7334), 378-381. Available from: https://doi.org/10.1038/nature09763

Myhre, G., Shindell, D., Breon, F., Collins, W., Fuglestvedt, J., Huang, J. et al. (2014) *Anthropogenic and Natural Radiative Forcing. In: Climate Change 2013: The Physical Science Basis. Contribution of Working Group I to the Fifth Assessment Report of the Intergovernmental Panel on Climate Change*. Cambridge University Press, Cambridge, United Kingdom and New York, NY, USA.

Nanding, N., Chen, Y., Wu, H., Dong, B.W., Tian, F.X., Lott, F. et al. (2020) Anthropogenic influences on 2019 July precipitation extremes over the mid–lower reaches of the Yangtze River. *Frontiers in Environmental Science*, **8**, 603601. Available from: https://doi.org/10.3389/fenvs.2020.603061

National Academies of Sciences, Engineering and Medicine. (2016) *Attribution of Extreme Weather Events in the Context of Climate Change.* Washington, DC: The National Academies Press.

Nie, J., Liu, P. & Zhao, C. (2021) Research on Relationship between Various Indexes of the Western North Pacific Subtropical High and Summer Precipitation in Eastern China (in Chinese). *Atmospheric Science,* **45**(4), 833-850. Available from: https://doi.org/10.3878/j.issn.1006-9895.2009.20160

O'Gorman, P. (2012) Sensitivity of tropical precipitation extremes to climate change. *Nature Geoscience*, **5**(10), 697-700. Available from: https://doi.org/10.1038/ngeo1568

O'Neill, B.C., Tebaldi, C., van Vuuren, D.P., Eyring, V., Friedlingstein, P., Hurtt, G. et al. (2016) The Scenario Model Intercomparison Project (ScenarioMIP) for CMIP6. *Geoscientific Model Development*, **9**(9), 3461-3482. Available from: https://doi.org/10.5194/gmd-9-3461-2016

Paik, S., Min, S.-K., Zhang, X., Donat, M. G., King, A. D. & Sun, Q. (2020). Determining the anthropogenic greenhouse gas contribution to the observed intensification of extreme precipitation. *Geophysical Research Letters*, **46**, e2019GL086875. Available from: https://doi.org/10.1029/2019GL086875

Papalexiou, S.M. & Koutsoyiannis, D. (2013) Battle of extreme value distributions: a global survey on extreme daily rainfall. *Water Resources Research*, **49**(1), 187-201. Available from: https://doi.org/10.1029/2012WR012557

Papalexiou, S.M. & Montanari, A. (2019) Global and Regional Increase of Precipitation Extremes Under Global Warming. *Water Resources Research*, **55**(6): 4901-4914. Available from: https://doi.org/10.1029/2018WR024067

Polson, D., Bollasina, M., Hegerl, G.C. & Wilcox, L.J. (2014) Decreased monsoon precipitation in the Northern Hemisphere due to anthropogenic aerosols. *Geophysical Research Letters*, **41**(16), 6023-6029. Available from: https://doi.org/10.1002/2014GL060811

Rayner, N.A., Parker, D.E., Horton, E.B., Folland, C.K., Alexander, L.V., Rowell, D.P. et al. (2003) Global analyses of sea surface temperature, sea ice, and night marine air temperature since the late nineteenth century, *Journal of Geophysical Research: Atmospheres*, **108**, 4407. Available from: https://doi.org/10.1029/2002JD002670

Rotstayn, L.D., Collier, M.A., Chrastansky, A., Jeffrey, S.J., & Luo, J. (2013) Projected effects of declining aerosols in RCP4.5: unmasking global warming? *Atmospheric Chemistry and Physics*, **13**(7), 10883-10905. Available from: https://doi.org/10.1029/2002JD002670

Song, F., Zhou, T., & Qian, Y. (2014) Responses of East Asian summer monsoon to natural and anthropogenic forcings in the 17 latest CMIP5 models. *Geophysical Research Letters,* **41**, 596– 603. Available from: https://doi.org/10.1002/joc.6887

Stott, P.A., Christidis, N., Otto, F.E.L., Sun, Y., Vanderlinden, J.P., van Oldenborgh, G.J. et al. (2016) Attribution of extreme weather and climate-related events. *WIREs Climate Change*, **7**, 23-41. Available from: https://doi.org/10.1002/wcc.380

Sun, Q. & Miao, C. (2018) Extreme Rainfall (R20mm, RX5day) in Yangtze–Huai, China, in June–July 2016: The Role of ENSO and Anthropogenic Climate Change. *Bulletin of the American Meteorological Society*, **99**(1), S102-S106. Available from:

https://doi.org/10.1175/BAMS-D-17-0091.1

Sun, Y., Dong, S.Y., Hu, T., Zhang, X. & Stott, P. (2019) Anthropogenic Influence on the Heaviest June Precipitation in Southeastern China since 1961. *Bulletin of the American Meteorological Society*, 100(1), S79-S83. Available from: https://doi.org/10.1175/BAMS-D-18-0114.1

Sun, Y., Zhang, X., Ding, Y., Chen, D., Qin, D. & Zhai, P. (2021) Understanding human influence on climate change in China. *National Science Review*, **9**(3), 113. Available from: https://doi.org/10.1093/nsr/nwab113

Tang, H., Wang, Z., Tang, B., Ma, Y., Pei, L., Tian, F. et al. (2022) Reduced probability of 2020 June–July persistent heavy Meiyu rainfall event in the mid-lower reaches of the Yangtze River basin under anthropogenic forcing. *Bulletin of the American Meteorological Society*, **103**(1), S83-S89. Available from: https://doi.org/https://doi.org/10.1175/BAMS-D-21-0167.1

Tang, Y., Huang, A., Wu, P., Huang, D., Xue, D. & Wu, Y. (2021) Drivers of summer extreme precipitation events over East China. *Geophysical Research Letters*, **48**, e2021GL093670. Available from: https://doi.org/10.1029/2021GL093670

Tao, L., Hu, Y. & Liu, J. (2016) Anthropogenic forcing on the Hadley circulation in CMIP5 simulations. *Climate Dynamics*, **46**(9), 3337-3350. Available from: https://doi.org/10.1007/s00382-015-2772-1

Teutschbein, C. & Seibert, J. (2012) Bias correction of regional climate model simulations for hydrological climate-change impact studies: Review and evaluation of different methods. *Journal of Hydrology*, **456-457**, 12-29. Available from: https://doi.org/10.1016/j.jhydrol.2012.05.052

Tian, F., Dong, B., Robson, J. & Sutton, R. (2018) Forced decadal changes in the East Asian summer monsoon: the roles of greenhouse gases and anthropogenic aerosols. *Climate Dynamics*. **51**, 3699–3715. Available from: https://doi.org/10.1007/s00382-018-4105-7

Vecchi, G.A., Soden, B.J., Wittenberg, A.T., Held, I.M., Leetmaa, A. & Harrison, M.J. (2006) Weakening of tropical Pacific atmospheric circulation due to anthropogenic forcing. *Nature*, **441**(7089), 73-76. Available from: https://doi.org/10.1038/nature04744

Wang, Y., Luo, Y. & Shafeeque, M. (2019) Using a Gaussian Function to Describe the Seasonal Courses of Monthly Precipitation and Potential Evapotranspiration across the Yellow River Basin, China. *Journal of Hydrometeorology*, **20**(11), 2185-2201. Available from:

https://doi.org/https://doi.org/10.1175/JHM-D-19-0019.1

Wang, Z. & Qian, Y. (2009) Frequency and intensity of extreme precipitation events in China (in Chinese). *Advances in Water Science*, **20**(1), 1-9. Available from: https://doi.org/10.3321/j.issn:1001-6791.2009.01.001

Wang, Z., Zhang, H. & Zhang, X. (2015) Simultaneous reductions in emissions of black carbon and co-emitted species will weaken the aerosol net cooling effect. *Atmospheric Chemistry and Physics*, **15**(7), 3671-3685. Available from: https://doi.org/10.5194/acp-15-3671-2015

Wang, Z., Zeng, Z., Lai, C., Lin, W., Wu, X. & Chen, X. (2017) A regional frequency analysis of precipitation extremes in Mainland China with fuzzy c-means and L-moments approaches. *International Journal of Climatology*, **37**, 429-444. Available from: https://doi.org/10.1002/joc.5013

Wang, Z., Sun, Y., Zhang, X., Li, T., Li, C., Min, S.-K. et al. (2023) Human influence on historical heaviest precipitation events in the Yangtze River Valley. *Environmental Research Letters*, **18**, 024044. Available from: https://doi.org/10.1088/1748-9326/acb563

Wu, Q.Y., Li, Q.Q., Ding, Y.H., Shen, X.Y., Zhao, M.C. & Zhu, Y.X. (2022) Asian summer monsoon responses to the change of land–sea thermodynamic contrast in a warming climate: CMIP6 projections. *Advances in Climate Change Research*, **13**(2), 205-217. Available from: https://doi.org/10.1016/j.accre.2022.01.001.

Xu, H., Chen, H. & Wang, H. (2022) Detectable Human Influence on Changes in Precipitation Extremes Across China. *Earth's Future*, **10**, e2021EF002409. Available from: https://doi.org/10.1029/2021EF002409

Xu, Y., Lamarque, J. & Sanderson, B. (2018) The importance of aerosol scenarios in projections of future heat extremes. *Climatic Change*, **146**(3), 393-406. Available from: https://doi.org/10.1007/s10584-015-1565-1

Yang, L., Villarini, G., Smith, J.A., Tian, F. & Hu, H. (2013) Changes in seasonal maximum daily precipitation in China over the period 1961 -2006. *International Journal of Climatology*, **33**(7), 1646-1657. Available from: https://doi.org/10.1002/joc.3539

Yang, Y., Ren, L., Wu, M., Wang, H., Song, F., Leung, R. et al. (2022) Abrupt emissions reductions during COVID-19 contributed to record summer rainfall in China. *Nature Communication*s. **13**, 95.

Available from: https://doi.org/10.1038/s41467-022-28537-9

Yuan, X., Wang, S. & Hu, Z. (2018) Do Climate Change and El Niño Increase the Likelihood of Yangtze River Extreme Rainfall? *Bulletin of the American Meteorological Society*, **99**(1), S113-S117. Available from: https://doi.org/10.1175/BAMS-D-17-0089.1

Zhang, L., Fu, T.M., Tian, H., Ma, Y., Chen, J.p., Tsai, T.C. et al. (2020) Anthropogenic aerosols significantly reduce mesoscale convective system occurrences and precipitation over Southern China in April. *Geophysical Research Letters.* **47**, e2019GL086204. Available from: https://doi.org/10.1029/2019GL086204

Zhang, Y., Wang, D. & Ren, X. (2008) Seasonal variation of the meridional wind in the temperate jet stream and its relationship to the Asian Monsoon. *Acta Meteorologica Sinica*, **24**, 446– 454.

Zhang, Q., Li, J., Singh, V.P. & Xu, C.Y. (2013) Copula-based Spatio-temporal patterns of precipitation extremes in China. *International Journal of Climatology*, **33**(5), 1140-1152. Available from: https://doi.org/10.1002/joc.3499

Zhang, W., Li, W., Zhu, L., Ma, Y., Yang, L., Lott, F.C. et al. (2020) Anthropogenic Influence on 2018 Summer Persistent Heavy Rainfall in Central Western China. *Bulletin of the American Meteorological Society*, **101**(1), S65-S70. Available from:https://doi.org/10.1175/BAMS-D-19-0147.1

Zhao, A., Stevenson, D. & Bollasina, M. (2019) The role of anthropogenic aerosols in future precipitation extremes over the Asian Monsoon Region. *Climate Dynamics*, **52**, 6257-6278. Available from: https://doi.org/10.1007/s00382-018-4514-7

Zhao, C., Tie, X. & Lin, Y. (2006) A possible positive feedback of reduction of precipitation and increase in aerosols over eastern central China. *Geophysical Research Letters*. **33**, L11814. Available from: https://doi.org/10.1029/2006GL025959

Zhou, T., Yu, R., Zhang, J., Drange, H., Cassou, C., Deser, C. et al. (2009). Why the Western Pacific Subtropical High Has Extended Westward since the Late 1970s. *Journal of Climate*, **22**(8), 2199-2215. Available from: https://doi.org/10.1175/2008JCLI2527.1

Zhou, C., Wang, K. & Qi, D. (2018) Attribution of the July 2016 Extreme Precipitation Event Over China's Wuhang. *Bulletin of the American Meteorological Society*, **99**(1), S107-S112. Available from:

https://doi.org/10.1175/BAMS-D-17-0090.1

Zhou, T., Ren, L. & Zhang, W. (2021) Anthropogenic influence on extreme Meiyu rainfall in 2020 and its future risk. *Science China Earth Sciences*, **64**, 1633–1644. Available from: https://doi.org/10.1007/s11430-020-9771-8